Chronology and provenance of the Yichang Gravel Layer deposits in the Jianghan Basin, middle Yangtze River Valley, China: Implications for the timing of channelization of the Three Gorges Valley

Chuanyi Wei, Pierre Voinchet, Yufen Zhang, Jean-Jacques Bahain, Chunru Liu, Chunguo Kang, Gongming Yin, Xilin Sun, Chang'An Li

Chronology and Provenance of the Yichang Gravel Layer deposits in the Jianghan Basin, Middle Yangtze River Valley, China: Implications for the Timing of Channelization of the Three Gorges Valley

Chuanyi Wei [1, 2, *], Pierre Voinchet [2], Yufen Zhang [3], Jean-Jacques Bahain [2], Chunru Liu [4], Chunguo Kang [5], Gongming Yin [4], Xilin Sun [1], Chang'an Li [1, 6, *]

1. School of Earth Sciences, China University of Geosciences, Wuhan 430074, China
2. Département de Préhistoire du Muséum National d'Histoire Naturelle, URM 7194 CNRS, 1 rue René Panhard, 75013 Paris, France
3. Institute of Geophysics and Geomatics, China University of Geosciences, Wuhan 430074, China
4. State Key Laboratory of Earthquake Dynamics, Institute of Geology, China Earthquake Administration, Beijing 100029, China
5. School of Geography and Tourism, Harbin University, Harbin 150086, China
6. State Key Laboratory of Biogeology and Environmental Geology, Wuhan 430074, China

*** Corresponding author at:** School of Earth Sciences, China University of

Geosciences, No. 388 Lumo Road, Wuhan, China, 430074

E-mail: chuanyiwei@cug.edu.cn (Chuanyi Wei)

Abstract：The Three Gorges Valley, linking the upper and the middle-lower Yangtze River areas is a key area for understanding the geomorphological evolution of the Yangtze River valley, especially the timing of its formation, which remains controversial and occurred following the authors to from the pre-Miocene to Late Pleistocene periods. The 100 m thick Yichang Gravel Layer (YGL), extending over an area >100 km^2, is immediately observed downstream of the Three Gorges Valley in the middle Yangtze River Basin also named Jianghan Basin. Studying heavy minerals assemblage and chronology of the YGL deposits can shed lights not only on the geological origin of the sediments and the morphological evolution of the Three Gorges Valley, but also the formation of the Yangtze River Valley. In this study, 18 sediment samples carried out from six representative sections of the unconsolidated YGL and 2 samples from the underlying Neogene and Paleogene bedrocks were analyzed in order to examine their heavy mineral assemblage compositions. These assemblages were compared with modern Yangtze River sediments sampled in Yichang area (n=5) and present-day sediments from other rivers of the Jianghan Basin (n=6) to further identify the sediment provenance of the YGL. The statistic results indicate that the heavy minerals identified the YGL dominated by zircon, epidote, titanite, hematite, limonite and ilmenite, are similar to the assemblages observed in the 5 modern Yangtze River sediment samples but differ obviously from both

underlying bedrock assemblages, containing kyanite, garnet, rutile and monazite, and other modern river sediments (Jianghan Basin), including hornblende, chlorite, tourmaline, rutile, anatase, spinel and garnet). In addition, 8 sandy samples from the YGL were dated by Electron Spin Resonance (ESR) method using Ti-Li center, showing a deposition age ranging between 1123±139 and 734±183 ka. Based on these observations, we propose that the YGL sediments derived from the upper Yangtze River Basin above the Three Gorges Valley, indicating that the Three Gorges Valley was channelized before 1.12 Ma ago. This result is consistent with previous provenance tracing studies of continuous deposited late Cenozoic sediment from central Jianghan Basin (since 3.0 Ma), which also constrains the incision time of the Three Gorges to ~1.1 Ma.

Keywords: Heavy mineral provenance tracing; Quartz Electron Spin Resonance (ESR) dating; Yichang Gravel Layer; Three Gorges Valley; the Yangtze River Basin

1. Introduction

The Yangtze River, is the most important river linking the Tibetan Plateau and the East China Sea (Fig. 1A). The Yangtze River, and its tributaries, delivers large volumes of water, sediments and associated chemical compounds from their headwater regions to its middle–lower reaches and the East China Sea. The river has

hence significantly influenced the evolution of the sedimentary system in its drainage basin and greatly affected the geomorphology, climate, and ecological environment of the whole East Asia (Zhang et al., 2014). It explains why the formation and evolution of the present-day Yangtze River has been a matter of great interest since the beginning of the 20th century (Lee, 1924). After a debate of more than 100 years, the First Bend near Shigu city on the SE Tibetan Plateau and the Three Gorges area, which links the upper and middle reaches of the river, have become recognized as two key areas for understanding the history of the geomorphological development of the Yangtze River (Fig. 1B; Clift et al., 2006; Xiang et al., 2007; Jia et al., 2010; Wang et al., 2013; Gu et al., 2014).

Recently, many studies, in particular on river terrace dating, bedrock uplift and denudation history, and surveys of the regional geology and geomorphologic evolution have been realized in order to establish the timing of Three Gorges Valley incision, yet estimated vary markedly. This timing remains strongly debated, with suggestions ranging between the Paleogene and Neogene periods (Clark et al., 2004; Richardson et al., 2010; Zheng et al., 2013), the early Pleistocene (Li et al., 2001; Kazumi, 2005; Yang et al., 2006; Xiang et al., 2007; Zhang et al., 2008; Kong et al., 2009; Wang et al., 2010; Gu et al., 2014), and the late Quaternary times (0.15–0.20 Ma; Gong et al., 1997; Brookfield et al., 1998; Chen et al., 2009). Until today, there is no consensus regarding the formation time of the Three Gorges Valley (Gu et al., 2014).

River terrace system can be used to directly reconstruct the capture history of the Three Gorges. However, strong tectonic activity in this area results in poor terrace system development and later geological processes destroyed the terrace depositional systems. In addition, the terrace sediments, consisting mainly in coarse detrital materials, are difficult to date. The terrace sediment system observed in the canyon area formed after the gorge incision, meaning that the dating results obtained on Yangtze River terraces are much younger than the estimates of the timing of Three Gorges incision. Furthermore, surveys of regional geology and geomorphological evolution are usually not sufficient to provide definitive age estimates.

Over the last two decades, tracing the sediment source has become an effective method to reconstruct river evolution and various approaches, such as geochemical and mineralogical analyses as well as environmental magnetism study, have been applied to trace the provenance of the Yangtze River Basin sediments (Clift et al., 2006; Yang et al., 2006; Xiang et al., 2007; Zhang et al., 2008; Huang et al., 2009; Kong et al., 2009; Jia et al., 2010; Richardson et al., 2010; Wang et al., 2010; Zheng et al., 2013; Gu et al., 2014; Wang et al., 2014; Zhang et al., 2014, 2017). However, most of those studies focused only on the middle–lower reaches or the delta area of the Yangtze River, far from the Three Gorges; consequently, typical river depositional systems directly related to the Three Gorges area have not yet been investigated.

Recently, electron spin resonance (ESR) dating has been successfully applied on fluvial sediments, using among others titanium (Ti) centers (Rink et al., 1997, 2007; Lin et al., 2006; Beerten et al., 2007; Tissoux et al., 2007; Voinchet et al., 2007, 2015;

Yin et al., 2007; Liu et al., 2010, 2015; Duval et al., 2017; Grün et al., 2018; Richter et al., 2019; Voinchet et al., 2019). Direct ESR dating of the Jianghan Basin sediments could help to constrain the formation time of the Three Gorges Valley. In addition, because a diversity of mineral species is found in the sediments and the factors affecting mineral assemblages are well understood, heavy mineral analysis offers a high-resolution approach to determining the origin of sand and hence sedimentary provenance (Morton et al., 1994, 1999; Garzanti and Ando, 2007; Yang et al., 2009; AndÒ et al., 2012; Hauptvogel et al., 2012).

The Yichang Gravel Layer (YGL) in the Jianghan Basin, located just downstream of the Three Gorges, is considered as the most informative deposit for elucidating the incision timing of the Three Gorges (Fig. 1B-C; Xiang et al., 2007; Zhang et al., 2017). In this study, we used heavy mineral assemblages of the Yichang Gravel Layer to constrain the sediment source. Additionally, ESR dating with Ti–Li center was carried out to identify deposition age of the YGL. Finally, we discuss the implications of our results for the timing of the Three Gorges incision.

Fig. 1

2. Geographical and geological background

2.1 The Yangtze River

The Yangtze River is the longest Asian river with 6380 km long, more than 700 tributaries and a catchment area of 1.8×10^6 km^2 (Fig. 1B and 2). The Yangtze River spans the regional structure of China with three-grade relief terraces and its curse can

be divided into three parts: the upper reaches, from its spring in the Qinghai Province to the city of Yichang; the middle reaches, between Yichang and the city of Hukou; and the lower reaches, from Hukou city to the East China Sea (Fig. 2; Shao et al., 2012). The river runs through several large catchment basins, including the Sichuan Basin, Jianghan Basin, Dongting Lake, Poyang Lake, and Taihu Lake, from the headwaters east to the estuary. The upper Yangtze River Valley, especially the mountainous regions in the Jinshajiang river and Jialingjiang river basins, experiences the strongest soil erosion and has the highest sediment production of any river system, up to 1000–1500 ton/$km^2 \cdot a$ (Yang et al., 2009).

Geologically, the Yangtze River River flows mainly on the Yangtze Craton surrounded by several geotectonic units (Fig. 2). The major tributaries of the upper–middle Yangtze River drainage areas run through regions with distinct tectonic histories and source bedrocks (Zhang et al., 2014). The upper Jinshajiang Valley contains hence metapsammites and metapelites, carbonate rocks, and acidic igneous rocks, notably intermediate–acidic rocks that were formed during the Miocene–Pliocene Himalayan orogeny. Paleozoic carbonate rocks and E'meishan Basalt are the major source rocks in the upper Yangtze River valley, each occupying an area of about 300×10^3 km^2. The middle and lower reaches of the Yangtze River are characterized by Paleozoic sedimentary rocks, Mesozoic intermediate–acidic igneous rocks, and Quaternary detrital sediments. The Mesozoic Yanshanian igneous rock belt crops out extensively along the main Yangtze River, whereas older low-to- medium-grade metamorphic rocks occur sporadically in the Poyang Lake Basin and Taihu Lake area

(Yang et al., 2009).

Fig. 2

2.2 The Three Gorges area and the Jianghan Basin

The Yangtze River which runs first through the Three Gorges and then through the Jianghan Basin, which as the first outlet of the Three Gorges contains the most important deposits for research on the incision onset and timing of the Three Gorges (Zhang et al., 2017). It is located and corresponds to an important catchment area, in which large amounts of material are deposited from the upper Yangtze reaches, with a deposition timing considered as quite continuous during the late Cenozoic or forming a continuous upper Cenozoic succession (Zhang et al., 2008). Hence, the Jianghan Basin provides ideal conditions to reconstruct the evolution of the Yangtze River.

2.3 Study area and sections

The Yichang Gravel Layer deposits, which form an inverted triangle shape mainly in the western Jianghan Plain immediately downstream of the Three Gorges, occur over an area of more than 100 km^2 (Fig. 1C). Because of its wide distribution and key geographical location, many representative sections of the Yichang Gravel Layer are critical for research of the stratigraphic succession, geomorphological evolution, and paleoenvironmental changes of the middle Yangtze River Basin, especially concerning on the incision history of the Three Gorges. Field investigations have demonstrated that the unconsolidated Yichang Gravel Layer direct unconformably covers following the zones either Neogene or Paleogene hard bedrocks and is recovered by the middle Pleistocene “vermicular red earth” (Deng et

al., 2018). The Neogene Duodaoshi formation is composed by lacustrine deposits, the Paleogene Pailoukou formation is composed by fluvio-lacustrine deposits. Li et al. (2001) showed that there are seven terraces well developed along the eastern Sichuan Basin and the Three Gorges, date from early to late Pleistocene (1.16 ~ 0.01 Ma). And the chronostratigraphic evidence and diagnostic sediments are generally comparable in spatial and temporal from the Sichuan Basin, through the Three Gorges, to the Jianghan Basin in their study.

The typical sequence of the Yichang Gravel Layer, more than 100 m thick, can be observed on three successive sections, which are from the oldest to the youngest the Lijiayuan Section, the Yunchi Section, and the Shanxiyao Section (Fig. 3) and represent a continuous detrital deposition phase. At the bottom of the seqeunce, the ~21 m thick Lijiayuan Section is at an elevation ranging from 69 to 90 m asl and the size of the gravel clasts becomes larger upwards, from 2–5 cm at the base to 5–30 cm at the top, while the sand lenses become increasingly thinner, the basal sand lens being more than 10 m thick; the Yunchi Section is about 60 m thick between 92 and 152 m asl, and it is mainly constituted by gravel layers with some sand lenses; finally the Shanxiyao Section, about 20 m thick with an elevation comprises between 152 and 173 m asl, consists mainly of thick gravel layers with some thin sand lenses. The sedimentary facies and depositional sequences of the Yichang Gravel Layer are summarized in Fig. 3.

Fig. 3

3. Sampling, methods, and experiments

3.1 Sampling

Eight sand lenses along the Yichang Gravel Layer sequence were sampled for ESR dating, as shown in Fig. 3. Before sampling, we horizontally removed a 20-cm-thick surface layer at each sampling site, and collected the sample in the middle part of each sand lens.

The resetting of the ESR Ti-Li signal in quartz prior to their deposits plays a key role in the accuracy of the results. Thus, in order to evaluate the efficiency of the zeroing (or bleaching) process in modern sediments, we have also collected and analyzed four scattered surface samples (indexed YCXD01, YCXD02, YCXD03, and YCXD04) from the present-day Yangtze River floodplain in the Yichang area.

In addition, to constrain the sediment provenance of the Yichang Gravel Layer deposits, 18 sediments were sampled from six typical localities, Miaopu, Jichanglu, Luyanchong, Shanxiyao, Yunchi, and Baiyangdu sections, for heavy mineral analyses (Fig. 4; Table 1; Kang et al., 2014). Furthermore, two samples were also collected from the underlying bedrocks, one in the Neogene Duodaoshi Formation (sample DDS-1) and one in the Paleogene Pailoukou Formation (sample PLK-1), also for heavy mineral examination (Table 1).

Fig. 4

Table 1

3.2 Heavy mineral analysis

The experimental procedure for heavy mineral analysis was as follows. First, the samples were dried and a 1-kg quantity was taken from each sample. These 1-kg samples were immersed in clear water for 48 hours, then sieved by compression and water elutriation to obtain the 0.125–0.063 mm fraction (Morton and Hallsworth, 1994; Morton et al., 2011). The samples were separated and weighed with an electronic balance after drying (accuracy 0.0001 g). Second, a 10-g sample was obtained by division for bromoform separation (density 2.89 g/cm^3) of the light and heavy minerals while flushing repeatedly with alcohol. After drying under a constant temperature of 60 °C, the portion of the sample containing the heavy minerals was weighed to obtain the heavy mineral content. Third, in the heavy mineral sample, 10 fields of view were selected stochastically using the strip method under a stereoscopic microscope for mineral identification, using the mean value to reduce error. Several samples were ground into slices for confirmation of mineral identifications under a polarizing microscope. More than 600 grains were identified for every heavy mineral sample and the percentage of each type of heavy mineral was calculated. As the heavy mineral samples were concentrates of the same size fraction, the particle percentage can be used to represent the volume percentage. Finally, as the proportion of each heavy mineral was known, the weight of each mineral could be calculated.

3.3 Electron spin resonance (ESR) dating

3.3.1 Sample preparation

In the present study, we have used the Ti–Li centers of quartz for sand ESR

dating of the Yichang Gravel Layer. Sample preparation followed the method described by Liu et al. (2010, 2015). Each sample was treated with 30% H_2O_2 for 24 hours to remove organic material, then washed and cleaned with distilled water. The samples were then treated with 40% HCl for 24 hours to remove carbonates, then again washed and cleaned with distilled water. Heavy minerals were removed by heavy liquid separation (2.7 g/cm^3) and magnetic minerals by mechanical magnetic selection. The remaining part of the sample was attacked with 40% HF for 40 minutes to remove feldspars and etch quartz grain, then treated again with 40% HCl for more than 4 hours to remove fluorides created by the HF attack, rinsed with distilled water to neutralize the acid and dried at low temperature (43 °C) for more than 24 hrs. X-ray diffraction analyses revealed that the quartz content of the eight samples was comprised after preparation between 97.19% and 99.99%.

3.3.2 Gamma-ray irradiation

Each quartz sample was divided into 14 aliquots for irradiation. Irradiation was performed using the ^{60}Co source of the Peking University laboratory, with a dose rate of 42.25 Gy/min. Thirteen of the 14 aliquots of each sample were irradiated, at doses of 100, 200, 400, 800, 1200, 1600, 2000, 2500, 3000, 5000, 6000, 7000, and 9000 Gy. The 14th aliquot was not irradiated and the its ESR intensity represents the natural signal recorded by the quartz sample along its geological history.

3.3.3 ESR measurement

ESR measurements were carried out on a BRUKER EPR041XG X-band spectrometer cooled to 77 K with liquid nitrogen in a finger Dewar at the State Key

Laboratory of Earthquake Dynamics, Institute of Geology, China Earthquake Administration. ESR measurements of Ti–Li centers were realized with a microwave power of 5 mW and a modulation amplitude of 0.16 mT. The Ti–Li center intensity was measured from the top of the peak at g = 1.979 to the bottom at g = 1.913 (Rink et al., 2007; Liu et al., 2010). For each sample, readings were obtained at six angles, and the average value was calculated to reduce the difference caused by the anisotropy of quartz.

3.3.4 Dose rate evaluation

The environmental dose rate during the burial period was calculated from the present-day concentrations of uranium (U), thorium (Th), and potassium (K) of each sediment sample (Aitken, 1998). U and Th contents were obtained using a thick source Daybreak 530 Model alpha counter. The potassium oxide content was determined by atomic absorption. The water content was measured as 8±5 wt%.

During field investigation, we observed that vermicular red earth covered the top of the Shanxiyao section. The thickness of this regional formation is known as higher than 30 m, but in recent decades, the vermicular red earth has been removed by local people to make bricks. We consider therefore in this study that the effect of cosmic dose was negligible for the YGL samples.

3.3.5 Equivalent dose calculation

In the literature several mathematical functions have been proposed to fit the growth curve of the ESR intensities according to the doses (Yokoyama et al., 1985; Duval et al., 2015a, 2015b, 2016; Voinchet et al., 2018), in the present work, the

equivalent doses of the YGL quartz were determined by fitting the ESR data set with an exponential function (Yokoyama et al., 1985) with Microcal OriginPro 8 software. This choice is justified by the fact that, the added maximal dose being lower or equal to 10000 Gy. The growth curve is uniformly increasing and the use of another function taking into account a decrease at high dose is not necessary.

The fitting function (Liu et al., 2015) is expressed by:

$$I=I_{sat}\times(1-\exp(-\lambda\times(D+D_E)))$$

where I is the intensity of the ESR signal of a sample irradiated at the dose D,

I_{sat} is the saturation intensity,

λ is the coefficient of sensitivity of the sample,

D_E is the equivalent dose.

4. Results

4.1 Heavy mineral assemblages

Eighteen species of heavy minerals (i.e., with a density greater than 2.89 g/cm^3) were detected in Yichang Gravel Layer deposits and underlying bedrocks (Fig. 5; Table 2). Overall, the samples collected from various sections of the Yichang Gravel Layer display similar heavy mineral assemblages (Fig. 5A-F; Kang et al., 2014). Zircon, epidote, hematite, limonite, titanite, ilmenite and magnetite are the main heavy minerals observed in the YGL deposits, the four first species being the most common. It seems indicate that the sediments sampled on the different sections of the Yichang Gravel Layer have the same source, supplying material of consistent

298 composition. On the other hand, the bedrock formations, Duodaoshi formation and
299 Pailoukou formation, show heavy mineral assemblages that are markedly different
300 from those of the Yichang Gravel Layer, sediments (Fig. 5G-H). Hence, zircon,
301 kyanite, leucoxene, rutile, monazite, ilmenite and magnetite are the dominant heavy
302 minerals of the Neogene Duodaoshi Formation, whereas the main heavy minerals of
303 the Paleogene Pailoukou Formation are zircon, apatite, tourmaline, garnet, leucoxene,
304 rutile, ilmenite and magnetite. Notably, kyanite, garnet, rutile, monazite and magnetite
305 can be used as diagnostic minerals of the bedrock formations, whereas epidote, and
306 fragments of E'meishan basalt detritus are found only in the Yichang Gravel Layer
307 deposits.

308 ***Fig. 5***

309 ***Table 2***

310 In addition, the proportions of heavy mineral species in the assemblages differ
311 between the underlying bedrock formations and the Yichang Gravel Layer deposits.
312 Seven groups of heavy mineral species were hence characterized (Fig. 5). Zircon
313 (group 1) and ilmenite (group 6) are both the main heavy mineral in Yichang Gravel
314 Layer and bedrocks, however zircon content is significantly lower in Yichang Gravel
315 Layer (4.4-16%) than in the bedrocks (12-24%) while the ilmenite average
316 percentages are similar in the both units (27%). The percentage of Group 2 (apatite,
317 tourmaline and kyanite) varied between 0.8% and 4.8% into Yichang Gravel Layer
318 and between 5.8% and 10.6% in the bedrocks. Epidote (group 3) percentage are much
319 higher in Yichang Gravel Layer (3.2-30.6%) than in bedrocks (0-0.4%). Group 4 is

constituted by garnet, leucoxene, rutile and monazite. Group 4 percentages are ranging from 5.7% to 16.5% and between 35.3% and 46.8% in Yichang Gravel Layer and bedrock, respectively. Finally, Hematite and limonite (forming group 5) represent a percentage of 15-26% in Yichang Gravel Layer while magnetite (Group 7) show important concentration in the bedrock with a proportion of 40%.

4.2 Electron Spin Resonance (ESR) chronology

4.2.1 ESR signal intensity in present-day sediments

The ESR Ti–Li intensity curves of the quartz extracted from the present-day Yangtze River sediments are smooth and flat, showing no peak within red rectangle (Fig. 6). This result indicates that the Ti-Li signal is completely bleached by sunlight exposure in quartz extracted from the present-day Yangtze River sediments. As the quartz grains extracted from sand lenses of the Yichang Gravel Layer were transported and deposited in a manner similar to the modern floodplain sediments, we estimate that the Ti–Li center signal intensity of the quartz was also zeroed prior to deposition.

Fig. 6

4.2.2 ESR dating of the Yichang Gravel Layer

The ESR growth curves of the eight samples collected from the Yichang Gravel Layer are displayed Fig. 7. The quartz ESR signal intensities significantly increased with increasing gamma ray dose. From stratigraphically lowest to highest sections, the equivalent doses (De) of quartz grains sampled from Lijiayuan (LJY01, LJY02),

Yunchi (YC01, YC02, YC03 and YC04) and Shanxiyao sections (SXY01, and SXY02) were 2919±362, 2531±330, 2527±389, 2634±621, 2472±364, 2478±320, 2206±281, and 2230±555 Gy, respectively. As the environmental dose rates are quite homogeneous for the YGL sediments, the depositional ages determined for the eight sand lens (Table 3) are older for the Lijiayuan sediments (1123±139 ka, LJY01; 1105±144 ka, LJY02), than those obtained for Yunchi section (1098±169 ka, YC01; 1045±246 ka, YC02; 1043±154 ka, YC03; 983±127 ka, YC04) and Shanxiyao sections (865±110 ka, SXY01; 734±183 ka, SXY02), respectively. We can observe, in addition, that the De values and ESR ages are mainly in good stratigraphical order and they does not show inversion within error ranges.

Table 3

Fig. 7

5. Discussion

5.1 Provenance of the Yichang Gravel Layer

5.1.1 Comparison between YGL heavy mineral assemblage and present-day fluvial sediment

To identify the source of the Yichang Gravel Layer sediments, the heavy mineral assemblages of the Yichang Gravel Layer deposits was compared with those of the underlying bedrocks, present-day Yangtze fluvial sediments in the Yichang area, other rivers sediments in the Jianghan Basin as well as with published heavy mineral assemblage results (Fig. 8 and Fig. 9) (Yang, 1988; Xiang et al., 2007; Kang et al.,

2009; Yang et al., 2009). The statistic results show that the heavy mineral assemblage of the Yichang Gravel Layer sediments is similar to that of present-day Yangtze fluvial sediments, but significantly differs from that of the underlying bedrock formations and from modern sediments carried out from other river floodplains in the Jianghan Basin, such as Qingjiang River, Zhanghe River, Jushui River, Manao River and Hanjiang Rivers (Fig. 9). These results seem to indicate that the main source of the Yichang Gravel Layer sediments was the upper Yangtze River Basin and the contribution of rivers in Jianghan Plain seems very limited. In fact, only the large volume of water resulting from the incision of the Three Gorges seems to be able to produce such a widespread thick accumulation of gravels, the water flows of the other rivers in Jianghan Plain being too low to form a such huge gravel alluvial fan. In addition, these results are consistent with the conclusions derived from both the studies of magnetic parameters (Zhang et al., 2008) and Pb isotopic compositions of detrital K-feldspars (Zhang et al., 2017).

Fig. 8

Fig. 9

5.1.2 Relationship between heavy mineral assemblage and source bedrock

Because the heavy mineral characteristics of a sediment are inherited mainly from the geological source and are unlikely to change with weathering and transportation, heavy mineral assemblages have long been regarded as sensitive indicators of the sediment source (Morton et al., 1999; Garzanti et al., 2005, 2006;

Garzanti and Ando, 2007; Yang et al., 2009; Hauptvogel and Passchier, 2012). Thus, comparison of principle minerals of YGL sediments with those recognized in the different bedrocks outcropping inside the upper Yangtze River Basin allows us to constrain the provenance of the YGL materials.

The main heavy mineral species identified in the gravel layers in the Yichang area (zircon, apatite, tourmaline, sphene, leucoxene, rutile and monazite) are common minerals in igneous rocks, especially in intermediate to acidic granites. Epidote and garnet are sourced mainly from metamorphic rocks, whereas hematite, limonite, ilmenite, and magnetite are derived from a variety of rocks.

According to geological maps (Fig. 2; China Geological Survey, 2004), meso-acidic granite occurs mainly within the Jinshajiang, Yalongjiang, Minjiang, and upper Jialingjiang drainage basins and the Huangling anticline, all located west of the Three Gorges area. Ultrabasic and basic gabbros are common in the E'meishan mountain area and the Shennongjia area. Intermediate–acidic extrusive rocks and pyroclastic rocks are widely distributed within the Sichuan Basin and the western Shennongjia area. Metamorphic rocks are exposed mainly in the Panzhihua area and the Minjiang, upper Jialingjiang, and Wujiang drainage basins. Sedimentary rocks are common around the Yangtze River Basin. Furthermore, vanadium–titanium–magnetite deposits crop out widely in the Panzhihua area of the upper Jinshajiang drainage basin. There are scattered occurrences of magnetite in the Minjiang drainage basin, and hematite and limonite are widely distributed in the Three Gorges area and the upper Wujiang drainage basin (Zhao et al., 2004; Wang and Zhang, 2008). These

occurrences of iron minerals were the sources of the high hematite and ilmenite concentrations in the Yichang Gravel Layer causing the main sources of the heavy minerals in the Yichang Gravel Layer are rocks in the upper Yangtze River Basin.

The E'meishan basalt, which occupies an area of ~300×10^3 km^2, is the only large volcanic igneous province in China (Xiao et al., 2003; Yang et al., 2009). Accordingly, the E'meishan basalt has been regarded as a characteristic rock of the Yangtze River Basin. Xiang et al. (2007) indicated that material from the E'meishan basalt does not occur in the Yichang Gravel Layer, but that fresh basaltic clasts are present in T4 and T5 terraces. For these authors, the presence of such basaltic clasts originating from an area to the west of the Three Gorges in Pleistocene terraces, but not in the Yichang Gravel Layer deposits indicate that the YGL material source is located at the east of the Three Gorges rather than from the upper Yangtze River Basin. Thus, previous workers assumed that the terraces were formed by the Yangtze River system after the river had cut through the gorges. However, E'meishan basalt detritus were recently found in the Yichang Gravel Layer sediments and in core samples of contemporaneous sediments from the Jianghan Basin (Yang et al., 2014). Consequently, based on our mineralogical data, we further propose that the materials in the Yichang Gravel Layer were derived from the upper Yangtze River Basin. This finding might indicate that the incision of the Three Gorges occurred before the deposition of the Yichang Gravel Layer.

5.2 Chronology of the YGL and its implication for the channelization timing of

the Three Gorges Valley

Field works showed that the sediment widely overlying the Yichang Gravel Layer in the Jianghan Plain corresponds to Vermicular Red Earth. Previous studies showed that this formation accumulated from early middle Pleistocene (Liu et al., 2008; Deng et al., 2018). As the Yichang Gravel Layer deposition zone is located immediately after and below the outlet of the Three Gorges and as our analyses indicate that the YGL sediment is sourced mainly from the upper Yangtze River Basin, the timing of deposition of the Yichang Gravel Layer could provide a direct constraint on the timing of incision of the Three Gorges. Thus, evidence of the beginning of the deposits indicate the already formation of the Three Gorges Valley. From our ESR dating results, we propose that the layer was deposited between 1123±139 ka and 734±183 ka. Thus, the Three Gorges was incised by the Yangtze River during the late Lower Pleistocene, before 1.12 Ma.

5.3 Evidence from the late Cenozoic (since 3.0 Ma) sedimentation in the central Jianghan Basin

Based on our provenance interpretation and chronological results obtained on the Yichang Gravel Layer sediments, a drainage evolution model of the Yangtze River can be proposed (Fig. 10). In this model, we cannot give details prior to the early Pleistocene because the Yichang Gravel Layer does not go deep enough in western hilly area of Jianghan Basin, leading to a stratigraphic gap between the Yichang Gravel Layer and the underlying Neogene bedrock. However, our results clearly

447 demonstrate that the Three Gorges was incised before 1.12 Ma. This proposal is
448 supported by the data derived from the study of the Zhoulao Core (Core ZL, Fig. 8)
449 obtained from central Jianghan Basin close to the Yichang Gravel Layer (Zhang et al.,
450 2008).

451 The magnetic stratigraphic framework of the 300.49 m long Core ZL established
452 by Zhang et al. (2008) (Fig. 11) indicates the record of the Brunhes-Matuyama
453 boundary (ca. 0.78 Ma) at 81 m depth while the Matuyama-Gauss boundary (ca. 2.58
454 Ma) is recorded at 250 m. This late Cenozoic (since 3.0 Ma B.P.) sedimentation
455 record in central Jianghan Basin seems continuous, without erosional hiatus (Zhang et
456 al., 2008).

457 ***Fig. 10***

458 In previous studies, many provenance indicators had been applied to trace
459 sediment provenance of the Core ZL to constrain the formation of the Three Gorges,
460 Fig. 11. Magnetic parameter analysis of the Core ZL (Zhang et al., 2008) showed that
461 the contents of coarse materials and stable magnetic minerals both increased
462 significantly above about 110 m depth. Meanwhile, the magnetic susceptibility of the
463 sediments, their saturation isothermal remanent magnetization and the magnetic
464 susceptibility values of anhysteretic remanent magnetism increased suddenly, at the
465 same depth, indicating an important adjustment event in water system of the Jianghan
466 Plain, and a great change of the sedimentary environment and material composition.
467 Combined with the paleomagnetic framework, Zhang et al. (2008) proposed that the
468 channelization timing of the Three Gorges Valley probably occurred between 1.17 and

1.12 Ma ago. Heavy mineral analysis from the Core ZL (Kang et al., 2009) revealed that at about 110 m the sedimentation is related to a river with a mineralogical signature similar to the modern Yangtze River. Pyroxenes contents of the Core ZL significantly changed at about 104 m (Yang et al., 2012) and trace element characteristics (Yuan et al., 2012) indicated that values of several proxies (∑REE, Y, Th, U, Th/Sc, Co/Th, La/Sc, Cr/Cu) became smaller above and upwards about 125 m depth, which has been interpreted as evidence that the Three Gorges was incised 1.25 Ma ago. After these studies, another works including bulk Nd isotopic analysis (Shao et al., 2012), detrital zircon U–Pb geochronology (Wang et al., 2010), Pb isotopic compositions of detrital K-feldspars (Zhang et al., 2017) and muscovite $^{40}Ar/^{39}Ar$ chronology (Sun et al., 2018) were also performed to trace the sediment provenance of the ZL Core. All those studies constrained the formation timing of the Three Gorges during the early Quaternary, providing hence solid evidence for supporting our results.

Fig. 11

5.4 Paleography evolution of the Three Gorges Valley and Jianghan Basin

Our provenance interpretation and chronology results of the Yichang Gravel Layer, allow the proposal of a reconstruction for the valley paleography evolution of the Three Gorges and Jianghan Basin in the upper-middle Yangtze River. Wang et al. (2018) considered that the Three Gorges is a drainage-divide during Late Cretaceous to Eocene (Ca. 100 Ma to Ca. 50 Ma) but Pb isotope compositions of detrital

K-feldspars of Neogene bedrock indicate that Jianghan Basin was still fed by local sources, like Huangling Massif, but not by the paleo-upper Yangtze River Basin deposits (Zhang et al., 2017). Combined with our ESR results, we propose that the incision time of the Three Gorges is older than 1.12 Ma, these previous results indicate that it is younger than late Neogene, (Fig. 10).

Our drainage evolution model shows that before the Three Gorges capture, sediments coming from the east of the Three Gorges were east-shed into the Jianghan Basin, whereas sediments from the west of the Three Gorges and paleo- upper Yangtze River Basin were drained into the Sichuan Basin (Fig. 10A and B). Lots of the sediment, predecessor materials of the Yichang Gravel Layer, were then deposited in Sichuan Basin. After the Three Gorges incision, part of these sediments were carried pass the Three Gorges, and accumulated in the western part of the Jianghan Basin to formed Yichang Gravel Layer (Fig. 10C and D). Thus far, the middle and lower Yangtze linked together to form the present-day Yangtze River Basin.

This interpretation of the incision of the Three Gorges is at odds with the post middle Pleistocene formation models (Zhao et al., 1996; Gong and Chen, 1997; Xiang et al., 2007; Wang et al., 2010; Chen et al., 2009) and ante Miocene formation models (Clark et al., 2004; Clift et al., 2008; Richardson et al., 2010; Zheng et al., 2013; Wang et al., 2018). However, our proposal of drainage evolution model is clearly consistent with many studies, suggesting that the Three Gorges incision time was of early Pleistocene age (Li et al., 2001; Fan et al., 2004; Xie et al., 2006; Yang et al., 2006; Ma et al., 2007; Shu et al., 2008; Zhang et al., 2008; Huang et al., 2009; Kong

et al., 2009; Jia et al., 2010; Li et al., 2010; Gu et al., 2014).

6. Conclusions

The analyze of the heavy mineral assemblages of sediments sampled on six representative sections of the Yichang Gravel Layer indicate that the heavy mineral assemblages of the Yichang Gravel Layer are similar to those of the tributaries, mainstream and source bedrocks of the upper Yangtze River Basin, but are markedly different from those of rivers and underlying bedrocks in the Jianghan Basin. Thus, the material of the Yichang Gravel Layer was sourced mainly from the upper Yangtze River Basin, west of the Three Gorges.

The results of 8 ESR Ti–Li center dating analyses constrain the deposition timing of the Yichang Gravel Layer between 1123±139 and 734±183 ka, in good agreement with the results of field lithostratigraphical investigations. From these results, we propose that the Three Gorges was incised before 1.12 Ma ago. This result is consistent with the provenance tracing studies of the contemporaneous sediments from central Jianghan Basin.

Acknowledgements: This work was supported by the National Science Foundation of China (No. 41671011 and 41877292). We also thank Dr. Fei Han and Jintang Qin for their valuable suggestions in paper organization.

References:

533 Aitken, M.J., 1998. Introduction to optical dating: the dating of Quaternary sediments
534 by the use of photon-stimulated luminescence. Clarendon Press, Oxford, England.
535 Ando, S., Garzanti, E., Padoan, M., Limonta, M., 2012. Corrosion of heavy minerals
536 during weathering and diagenesis: A catalog for optical analysis. Sedimentary
537 Geology 280, 165-178. DOI: 10.1016/j.sedgeo.2012.03.023.
538 Beerten, K., Stesmans, A., 2007. ESR dating of sedimentary quartz: Possibilities and
539 limitations of the single-grain approach. Quaternary Geochronology 2, 373-380.
540 DOI: 10.1016/j.quageo.2006.03.003.
541 Brookfield, M.E., 1998. The evolution of the great river systems of southern Asia
542 during the Cenozoic India-Asia collision: rivers draining southwards.
543 Geomorphology 22, 285-312. DOI: 10.1016/S0169-555X(97)00082-2.
544 Chen, J., Wang, Z., Chen, Z., Wei, Z., Wei, T., Wei, W., 2009. Diagnostic heavy
545 minerals in Plio–Pleistocene sediments of the Yangtze Coast, China with special
546 reference to the Yangtze River connection into the sea. Geomorphology 113,
547 129-136. DOI: 10.1016/j.geomorph.2009.03.010.
548 China Geological Survey, 2004. Geological Map of China (1:2,500,000). China
549 Geological Map Press, Beijing (in Chinese).
550 Clark, M.K., Schoenbohm, L.M., Royden, L.H., Whipple, K.X., Burchfiel, B.C.,
551 Zhang, X., Tang, W., Wang, E., Chen, L., 2004. Surface uplift, tectonics, and
552 erosion of eastern Tibet from large-scale drainage patterns. Tectonics 23. DOI:
553 10.1029/2002tc001402.
554 Clift, P.D., Blusztajn, J., Nguyen, A.D., 2006. Large-scale drainage capture and

surface uplift in eastern Tibet-SW China before 24 Ma inferred from sediments of the Hanoi Basin, Vietnam. Geophysical Research Letters 33, 1-4. DOI: 10.1029/2006GL027772.

Clift, P.D., Long, H.V., Hinton, R., Ellan, R.M., Hannigan, R., Tan, M., Blausztajn, J., Duc, A., 2008. Evolving East Asian river systems reconstructed by trace element and Pb and Nd isotope variations in modern and ancient Red River-song Hong sediments. Geochemistry, Geophysics, Geosystems 9, Q04039. http://dx.doi.org/10.1029/2007GC001867.

Deng, C.L., Hao, Q.Z., Guo, Z.T., Zhu, R.X., 2018. Quaternary strata in China mainly comprise continental deposits in a variety of depositional settings. Science China Series D 48. DOI: 10.1360/N072017-00269.

Duval, M., Guilarte, V., 2015a. ESR dosimetry of optically bleached quartz grains extracted from Plio-Quaternary sediment: Evaluating some key aspects of the ESR signals associated to the Ti-centers. Radiation Measurements 78, 28-41. DOI: 10.1016/j.radmeas.2014.10.002.

Duval, M., Sancho, C., Calle, M., Guilarte, V., Peña-Monné, J.L., 2015b. On the interest of using the multiple center approach in ESR dating of optically bleached quartz grains: Some examples from the Early Pleistocene terraces of the Alcanadre River (Ebro basin, Spain). Quaternary Geochronology 29, 58-69. https://doi.org/10.1016/j.quageo.2015.06.006.

Duval, M., Arnold, L., Guilarte, V., Demuro, M., Santonja, M., Pérez-Gonzalez, A., 2016. Electron spin resonance dating of optically bleached quartz grains from the

Middle Palaeolithic site of Cuesta de la Bajada (Spain) using the multiple centres approach. Quaternary Geochronology 37, 82-96. DOI: 10.1016/j.quageo.2016.09.006.

Fan, D.D., Li, C.X., Yokoyama, K., Zhou, B.C., Li, B.H., Wang, Q., Yang, S.Y., Deng, B., Wu, G.X., 2004. Monazite age spectra in the late Cenozoic strata of the Changjiang delta and its implication on the Changjiang run-through time. Science China Series D 34, 1015–1022. DOI: 10.1360/01YD0447.

Garzanti, E., Andò, S., 2007. Chapter 20 Heavy Mineral Concentration in Modern Sands: Implications for Provenance Interpretation. Developments in Sedimentology 58, 517-545. DOI: 10.1016/S0070-4571(07)58020-9.

Garzanti, E., Andò, S., Vezzoli, G., Megid, A., Kammar, A.E., 2006. Petrology of Nile River sands (Ethiopia and Sudan): Sediment budgets and erosion patterns. Earth and Planetary Science Letters 252, 327-341. DOI: 10.1016/j.epsl.2006.10.001.

Garzanti, E., Vezzoli, G., Andò, S., Paparella, P., Clift, P.D., 2005. Petrology of Indus River sands: a key to interpret erosion history of the Western Himalayan Syntaxis. Earth and Planetary Science Letters 229, 287-302. DOI: 10.1016/j.epsl.2004.11.008.

Gong, S.Y., Chen, G.J., 1997. Evolution of Quaternary riversand lakes inthe middle reaches of the Yangtze River and its effect on the environment. Earth Science Journal of China University of Geosciences 22, 199–203 (in Chinese with English abstract).

Grun, R., 2018. A very personal, 35 years long journey in ESR dating. Quaternary

International, DOI: https://doi.org/10.1016/j.quaint.2018.11.038.

Gu, J.W., Chen, J., Sun, Q.L., Wang, Z.H., Wei, Z.X., Chen, Z.Y., 2014. China's Yangtze delta: Geochemical fingerprints reflecting river connection to the sea. Geomorphology 227, 166-173. DOI: 10.1016/j.geomorph.2014.05.015.

Hauptvogel, D.W., Passchier, S., 2012. Early–Middle Miocene (17–14 Ma) Antarctic ice dynamics reconstructed from the heavy mineral provenance in the AND-2A drill core, Ross Sea, Antarctica. Global and Planetary Change 82-83, 38-50. DOI: 10.1016/j.gloplacha.2011.11.003.

Huang, X.T., Zheng, H.B., Yang, S.Y., Xie, X., 2009. Investigation of sedimentary geochemistry of core DY03 in the Yangtze Delta: implication to tracing provenance. Quaternary Science 29, 299–307 (in Chinese with English abstract). DOI: 1001-7410(2009)02-299-09.

Jia, J.T., Zheng, H.B., Huang, X.T., Fu, Y., Yang, S.Y., 2010. Detrital zircon U-Pb ages of Late Cenozoic sediments from the Yangtze delta: Implication for the evolution of the Yangtze River. Chinese Science Bulletin 55, 1520-1528. DOI: 10.1007/s11434-010-3091-x.

Kang, C.G., Li, C.A., Wang, J.T., Shao, L., 2009. Heavy Minerals Characteristics of Sediments in Jianghan Plain and its Indication to the Forming of the Three Gorges. Earth Science Journal of China University of Geosciences 34, 419-427 (in Chinese with English abstract). DOI: 10.3321/j.issn:1000-2383.2009.03.006.

Kang, C.G., Li, C.A., Zhang, Y.F., Shao, L., Jiang, H.J., 2014. Heavy mineral Characteristics of the Yichang Gravel Layers and Provenance Tracing. Acta

Geologica Sinica 88, 254-262 (in Chinese with English abstract).

Kazumi, Y., 2005. Monazite age spectra in the Late Cenozoic strata of the Changjiang delta and its implication on the Changjiang run-through time. Science China 48, 5527-5532. DOI: 10.1360/01YD0447.

Kong, P., Granger, D.E., Wu, F.Y., Caffee, M.W., Wang, Y.J., Zhao, X.T., Zheng, Y., 2009. Cosmogenic nuclide burial ages and provenance of the Xigeda paleo-lake: Implications for evolution of the Middle Yangtze River. Earth and Planetary Science Letters 278, 131-141. DOI: 10.1016/j.epsl.2008.12.003.

Lee, J.S., Chao, Y.T., 1924. Geology of the Gorge District of the Yangtze (from Yichang to Tzekuei) with Special Reference to the Development of the Gorges. Acta Geologica Sinica-English Edition 3, 351-392. DOI: 10.1111/j.1755-6724.1924.mp33-4004.x.

Li, J.J., Xie, S., Kuang, M., 2001. Geomorphic evolution of the Yangtze Gorges and the time of their formation. Geomorphology 41, 125-135. DOI: 10.1016/S0169-555X(01)00110-6.

Li, T., Li, C.A., Kang, C.G., Lei, W.D., Yang, J., Wang, J.T., 2010. Sedimentary environment and geomorphological significance of the gravel bed in Yichang. Geology in China 37, 438–445, (in Chinese with English abstract). DOI:1000-3657(2010)02-0438-08.

Lin, M., Yin, G.M., Ding, Y., Cui, Y., Chen, K., Wu, C., Xu, L., 2006. Reliability study on ESR dating of the aluminum center in quartz. Radiation Measurements 41, 1045-1049. DOI: 10.1016/j.radmeas.2006.05.019.

643 Liu, C.C., Xu, X.M., Yuan, B.Y., Deng, C.L., 2008. Magnetostratigraphy of the
644 Qiliting section (SE China) and its implication for geochronology of the red soil
645 sequences in southern China. Geophysical Journal of the Royal Astronomical
646 Society 174, 107-117. DOI: 10.1111/j.1365-246X.2008.03814.x.
647 Liu, C.R., Yin, G.M., Gao, L., Bahain, J.J., Li J.P., Lin, M., Chen, S.M., 2010. ESR
648 dating of Pleistocene archaeological localities of the Nihewan Basin, North China –
649 Preliminary results. Quaternary Geochronology 5, 385-390. DOI:
650 10.1016/j.quageo.2009.05.006.
651 Liu, C.R., Yin, G.M., Han, F., 2015. Effects of grain size on quartz ESR dating of Ti–
652 Li center in fluvial and lacustrine sediments. Quaternary Geochronology 30,
653 513-518. DOI: 10.1016/j.quageo.2015.02.007.
654 Ma, Y.F., Li, C.A., Wang, Q.L., Yang, Y., Chen, G.J., Jiao, H.M., 2007. Statistics of
655 gravels from a bore in Zhoulao Town, Jianghan Plain and its relationship with
656 cut-through of the Yangtze 3-Gorges, China. Geological Science and Technology
657 Information 26, 40-44 (in Chinese with English abstract). DOI:
658 1000-7849(2007)02-0040-05.
659 Morton, A.C., Hallsworth, C., 1994. Identifying provenance-specific features of
660 detrital heavy mineral assemblages in sandstones. Sedimentary Geology 90,
661 241-256. DOI: 10.1016/0037-0738(94)90041-8.
662 Morton, A.C., Hallsworth, C.R., 1999. Processes controlling the composition of heavy
663 mineral assemblages in sandstones. Sedimentary Geology 124, 3-29.
664 DOI:10.1016/S0037-0738(98)00118-3.

665 Morton, A.C., Meinhold, G., Howard, J.P., Phillips, R.J., Strogen, D., Abutarruma, Y.,
666 Elgadry, M., Thusu, B., Andrew, G., Abutarruma, Y., 2011. A heavy mineral study
667 of sandstones from the eastern Murzuq Basin, Libya: constraints on provenance and
668 stratigraphic correlation. Journal of Africa Earth Sciences 61, 308-330. DOI:
669 10.1016/j.jafrearsci.2011.08.005.
670 Richardson, N.J., Densmore, A.L., Seward, D., Wipf, M., Li, Y., 2010. Did incision of
671 the Three Gorges begin in the Eocene? REPLY. Geology 38, 551-554. DOI:
672 10.1130/G30527.1.
673 Richter, M., Tsukamoto, S., Long, H., 2019. ESR dating of Chinese loess using the
674 quartz Ti centre: A comparison with independent age control. Quaternary
675 International, DOI: https://doi.org/10.1016/j.quaint.2019.04.003.
676 Rink, W.J., Bartol,l J., Schwarcz, H.P., Shane, P., Bar-Yosef, O., 2007. Testing the
677 reliability of ESR dating of optically exposed buried quartz sediments. Radiation
678 Measurements 42, 1618-1626. DOI: 10.1016/j.radmeas.2007.09.005.
679 Rink, W.J., Schwarcz, H.P., Lee, H.K., Valdés, V.C., Quirós, F.B.D., Hoyos, M., 1997.
680 ESR dating of Mousterian levels at El Castillo Cave, Cantabria, Spain. Journal of
681 Archaeological Science 24, 593-600. DOI: 10.1006/jasc.1996.0143.
682 Shao, L., Li, C.A., Yuan, S., Kang, C., Wang, J., Li, T., 2012. Neodymium isotopic
683 variations of the late Cenozoic sediments in the Jianghan Basin: Implications for
684 sediment source and evolution of the Yangtze River. Journal of Asian Earth
685 Sciences 45, 57-64. DOI: 10.1016/j.jseaes.2011.09.018.
686 Shu, Q., Zhang, M.H., Zhao, Z.J., Chen, H., Li, J.J., 2008. Sedimentary record from

the XH-1 core in North Jiangsu Basin and its implication on the Yangtze River run-through time. Journal of Stratigraphy 32, 308–314 (in Chinese with English abstract). DOI: 0253-4959(2008)03-0308-07.

Sun, X.L., 2018. Provenance and Evolution of the Yangtze River constrained by Detrital Minerals. Vrije Universiteit Amsterdam.

Tissoux, H., Falguères, C., Voinchet, P., Toyoda, S., Bahain, J.J., Despriée, J., 2007. Potential use of Ti-center in ESR dating of fluvial sediment. Quaternary Geochronology 2, 367-372. DOI: 10.1016/j.quageo.2006.04.006.

Voinchet, P., Falguères, C., Tissoux, H., Bahain, J.J., Despriée, J., Pirouelle, F., 2007. ESR dating of fluvial quartz: Estimate of the minimal distance transport required for getting a maximum optical bleaching. Quaternary Geochronology 2, 363-366. DOI: 10.1016/j.quageo.2006.04.010.

Voinchet, P., Toyoda, S., Falguères, C., Hernandez, M., Tissoux, H., Moreno, D., Bahain, J.J., 2015. Evaluation of ESR residual dose in quartz modern samples, an investigation on environmental dependence. Quaternary Geochronology 30, 506-512. DOI: 10.1016/j.quageo.2015.02.017.

Voinchet, P., Yin, G.M., Falguères, C., Liu, C.R., Han, F., Sun, X.F., Bahain, J.J., 2019. Dating of the stepped quaternary fluvial terrace system of the Yellow River by electron spin resonance (ESR). Quaternary Geochronology. DOI: 10.1016/j.quageo.2018.08.001.

Wang, J.T., Li, C.A., Yang, Y., Shao, L., 2010. Detrital zircon geochronology and provenance of core sediments in Zhoulao Town, Jianghan Plain, China. Journal of

709 Earth Science 21, 257-271. DOI: 10.1007/s12583-010-0090-4.
710 Wang, P., Zheng, H.B., Chen, L., Chen, J., Xu, Y., Wei, X., Yao, X., 2013.
711 Exhumation of the Huangling anticline in the Three Gorges region: Cenozoic
712 sedimentary record from the western Jianghan Basin, China. Basin Research 26,
713 505–522. DOI: 10.1111/bre.12047.
714 Wang, P., Zheng, H.B., Liu, S.F., Hoke, G., 2018. Late Cretaceous drainage
715 reorganization of the Middle Yangtze River. Geological Society of America
716 Bulletin. https://doi.org/10.1130/L695.1.
717 Wang, X.F., Zhang, X.R., 2008. Major Types of Iron Deposits in Sichuan and Their
718 Range of Reconnaissance. Acta Geological Sichuan 28, 287-304. (in Chinese with
719 English abstract) DOI: 1006-0995（2008）04-0287-03.
720 Xiang, F., Zhu, L.D., Wang, C.S., Zhao, X.X., Chen, H.D., 2007. Quaternary sediment
721 in the Yichang area: Implications for the formation of the Three Gorges of the
722 Yangtze River. Geomorphology 85, 249-258. DOI:
723 10.1016/j.geomorph.2006.03.027.
724 Xiao, L., Xu, Y.G., He, B., 2003. Emei mantle plume-subcontinental lithosphere
725 Interaction: Sr–Nd and O Isotopic Evidences from low-Ti and high-Ti basalts.
726 Journal of China University 9, 210-217. DOI: 1006-7493(2003)02-207-11.
727 Xie, S.Y., Yuan, D.X., Wang, J.L., Kuang, M.S., 2006. Features of the plantation
728 surface in the surrounding area of the Three Gorges of Yangtze. Carsologica Sinica
729 25, 40-45 (in Chinesewith English abstract). DOI:1001- 4810(2006)01- 0040- 06.
730 Yang, D.Y., 1988. Genetic mechanism of the alluvial terraces along the Three Gorges

course of the Changjiang River. Acta Geography Sinica 4, 120-126 (in Chinese with English abstract).

Yang, J., L,i C.A., Dembele, N.J., Jiang, H.J., 2014. Emeishan Basalts as provenance indicators: implications for formation of the Three Gorges. Earth Science Journal of China University of Geosciences 39, 431-442. DOI: 1000-2383(2014)04-0431-12.

Yang, J., Li, C.A., Zhang, Y.F., Kang, C.G., Shao, L., 2012. Ti-Augite in sediment of the Jianghan Plain as tracing mineral: implication for the evolution of the Yangtze River. Earth Science Journal of China University of Geosciences 37, 43-49 (in Chinese with English abstract). DOI: 10.3799/dqkx.2012.S1.005.

Yang, S., Li, C., Yokoyama, K., 2006. Elemental compositions and monazite age patterns of core sediments in the Changjiang Delta: Implications for sediment provenance and development history of the Changjiang River. Earth and Planetary Science Letters 245, 762-776. DOI: 10.1016/j.epsl.2006.03.042.

Yang, S., Wang, Z., Guo, Y., Li, C., Cai, J., 2009. Heavy mineral compositions of the Changjiang (Yangtze River) sediments and their provenance-tracing implication. Journal of Asian Earth Sciences 35, 56-65. DOI: 10.1016/j.jseaes.2008.12.002.

Yin, G.M., Bahain, J.J., Shen, G., Tissoux, H., Falguères, C., Dolo, J.M., Han, F,, Shao, Q., 2011. ESR/U-series study of teeth recovered from the palaeoanthropological stratum of the Dali Man site (Shanxi Province, China). Quaternary Geochronology 6, 98-105. DOI: 10.1016/j.quageo.2010.04.001.

Yuan, S.Y., Li, C.A., Zhang, Y.F., Shao, L., Kang, C.G., 2012. Trace element characteristics of sediments in Jianghan Basin: implications for expansion of the

753 upper reaches of the Yangtze River. Geology in China 39, 1042-1048 (in Chinese
754 with English abstract). DOI: 1000-3657(2012)04-1042-07.
755 Zhang, Y.F., Li, C.A., Wang, Q.L., Liang, C., Ma, Y.F., Kang, C.G., 2008. Magnetism
756 parameters characteristics of drilling deposits in Jianghan Plain and indication for
757 forming of the Yangtze River Three Gorges. Chinese Science Bulletin 53, 584-590.
758 DOI: 10.1007/s11434-008-0111-1.
759 Zhang, Z.J., Daly, J.S., Li, C.A., Tyrrell, S., Sun, X.L., Yan, Y., 2017. Sedimentary
760 provenance constraints on drainage evolution models for SE Tibet: Evidence from
761 detrital K-feldspar. Geophysical Research Letters 44. DOI:
762 10.1002/2017GL073185.
763 Zhang, Z.J., Tyrrell, S., Li, C.A., Daly, J.S., Sun, X.L., Li, Q.W., 2014. Pb isotope
764 compositions of detrital K‐feldspar grains in the upper-middle Yangtze River
765 system: Implications for sediment provenance and drainage evolution.
766 Geochemistry Geophysics Geosystems 15, 2765-2779. DOI:
767 10.1002/2014GC005391.
768 Zhao, C., 1996. River capture and origin of the Yangtze Gorges. Journal of
769 Changchun University Earth Sciences 26, 428-433 (in Chinese with English
770 abstract). DOI: 10.13278 /j.cnki . jjuese.1996.04.013.
771 Zhao, Y.M., Wu, L.S., 2004. Metallogenic regularity of major metal deposits in China.
772 Geology Press, Beijing.
773 Zheng, H.B., Clift, P.D., Wang, P., Tada, R., Jia, J.T., He, M.Y., Jourdan, F., 2013.
774 Pre-Miocene birth of the Yangtze River. Proceedings of the National Academy of

775 Sciences 110, 7556-7561. DOI: 10.1073/pnas.1216241110.

Table 1. Details of samples used in heavy mineral analysis of the Yichang Gravel Layer and the underlying bedrock

No.		Section	Samples	Location and elevation		
				Latitude (N)	Longitude (E)	Elevation (m)
1	YGL	Miaopu	SWMP-1, SWMP-2	30°41′78.3″	111°18′12.7″	130±5
2		Jichanglu	JCL-1, JCL-2, JCL-3	30°25′26.5″	111°27′20.6″	110±5
3		Luyanchong	LYC-1, LYC-2	30°32′44.8″	111°26′32.2″	110±5
4		Shanxiyao	SXY-1, SXY-2; SXY-3, SXY-4	30°28′53.4″	111°27′38.76″	155±5
5		Yunchi	YC-1, YC-2, YC-3, YC-4	30°28′52.3″	111°27′30.12″	92±5
6		Baiyangdu	BYD-1, BYD-2, BYD-3	30°25′78.4″	111°30′66.8″	87±5
7	Underlying bedrock	Duodaoshi Formation	DDS-1	30°34′01.79″	111°24′16.85″	104±5
8		Pailoukou Formation	PLK-1	30°22′20.59″	111°26′01.13″	47±5

Table 2. Heavy mineral species and percentage content (%) of the Yichang Gravel Layer and its bedrocks

Sampling section	Sample No.	zircon	apatite	tourmaline	sphene	kyanite	epidote	hornblende	pyroxene	garnet	leucoxene	rutile	monazite	anatase	Hematite and limonite	ilmenite	magnetite	allanite	detrital
Luyanchong section	LYC01	11.89	▲	0.71	1.56	▲	5.47	0	0	0.89	6.38	2.07	0	0.89	5.37	47.17	14.96	0	2.64
	LYC02	4.43	0.09	0.79	0.87	0	29.67	▲	▲	0.30	4.07	0.12	0	0.99	35.94	5.85	3.85	0.49	12.54
Miaopu section	MP01	5.04	1.64	1.87	0.32	1.33	3.98	▲	0	1.99	14.1	0.42	0	0.36	16.82	49.72	0.94	▲	1.48
	MP02	15.23	3.70	1.12	0.50	0	2.35	0	▲	0.28	3.76	2.3	0	2.82	30.78	35.54	1.1	0	0.53
Jichanglu section	JCL01	19.41	0.88	1.54	1.70	0	6.80	0	▲	0.97	11.9	3.38	0	0.97	31.53	7.98	0	▲	12.94
	JCL02	11.26	0.37	0.80	0.35	0	18.65	0	▲	1.01	7.25	0.71	0	1.01	6.1	33.35	2.62	▲	16.52
	JCL03	18.18	0.41	0.72	0.80	0	6.37	0	0	1.81	3.72	3.17	0	1.82	6.56	44.87	8.21	0	3.37
Yunchi section	YC01	2.25	0.92	0.40	1.77	0	20.43	5.05	0.88	2.02	2.07	1.18	0	1.01	41.48	3.57	1.31	0.5	12.77
	YC02	9.75	0.08	0.35	0.77	0	6.92	0	0	0.09	1.79	0.20	0	1.75	51.71	5.15	18.1	0.09	3.25
	YC03	3.36	0.55	0.80	0.88	▲	42.41	0.25	0.26	2.01	4.12	0.70	0	▲	4.85	33.18	2.6	0.2	2.24
	YC04	2.33	0.95	0.67	1.84	0	52.45	0	▲	2.09	6.44	0.24	0	▲	5.05	19.74	2.71	▲	4.67
Shanxiyao section	SXY01	8.87	4.09	0.10	0.56	0.11	8.80	0.10	0.11	1.28	12.9	0.75	0	0.38	32.38	22.99	0.2	▲	6.39
	SXY02	1.96	▲	0.07	0.56	0	6.97	0	▲	1.76	7.23	0.31	0	0.09	29.78	25.97	21.67	▲	4.19
	SXY03	13.73	3.48	3.04	▲	0.19	0.53	▲	0.18	0.20	8.45	1.68	0	6.86	31.83	23.03	0.78	0.25	5.05
	SXY04	2.15	0.88	▲	0	▲	13.53	▲	▲	2.89	27.62	1.12	0	▲	40.65	2.27	0	0	4.29
Baiyangdu section	BYD01	4.27	0.82	0.35	2.37	1.04	9.91	▲	0.79	2.70	2.08	1.84	0	▲	24.5	43.34	0.29	0	5.20
	BYD02	6.07	1.02	0.15	0.79	0.52	10.25	0.16	▲	1.50	5.20	2.19	0	0.37	23.62	45.91	0	0	2.24
	BYD03	3.00	2.45	0.43	0.79	0.33	7.10	0.37	▲	0.45	0.92	1.05	0	2.70					
Pailoukou	PLK01	23.89	0	0.12	1.03	5.61	0.37	0	0.12	0.85	8.11	10.77	15.54	0.59	3.76	29.25	39.48	0	10.03

Formation																		
Duodaoshi Formation	DDS01	11.89	5.03	4.01	1.95	1.60	0	0	0	16.62	20.96	9.19	0	0.74	1.15	25.71	39.44	0	10.57

▲ indicates that the mineral occasionally appeared in bulk sample. The YGL data were cited from Kang et al. (2014).

Table 3. ESR dating results of quartz Ti–Li centers from the Yichang Gravel Layer, Jianghan Basin

Sample No.	Depth (m)	U (ppm)	Th (ppm)	K_2O (%)	WT (%)	Environmental dose rate (Gy/ka)	Equivalent dose (Gy)	Age (ka)
SXY02	4	2.32	4.61	1.78	8±5	3.04	2230±555	734±183
SXY01	19	1.33	4.35	1.68	8±5	2.55	2206±281	865±110
YC04	40	0.878	5.82	1.66	8±5	2.52	2478±320	983±127
YC03	51	1.05	4.71	1.56	8±5	2.37	2472±364	1043±154
YC02	63	1.28	4.69	1.63	8±5	2.52	2634±621	1045±246
YC01	75	0.944	4.87	1.51	8±5	2.30	2527±389	1098±169
LJY02	83	1.08	5.53	1.37	8±5	2.29	2531±330	1105±144
LJY01	99	1.52	4.63	1.62	8±5	2.60	2919±362	1123±139

Figure 1. Location of the Yangtze River Basin and distribution of the Yichang Gravel Layer. A). The Yangtze River Basin acts as a linkage between the Tibetan Plateau and East China Sea; B). key capture points of the Yangtze River Basin: the First Bend (black circle) and the Three Gorges (red rectangle); and location of the Jianghan Basin at the outlet of the Three Gorges; C). distribution of the Yichang Gravel Layer (dashed line) and locations of the studied sections.

Figure 2. Map showing the bedrock and geological blocks in the Yangtze River Basin.

Figure 3. Elevation, lithological sequence, ESR sample locations, and field photographs of the studied sections.

Figure 4. Sedimentary logs of the sampling sites in the Yichang Gravel Layer, with the locations of individual samples marked (modified from Kang et al., 2014).

Figure 5. Main heavy mineral percentage of various sections of Yichang Gravel Layer (YGL) and its bedrocks. Zircon, epidote, hematite and limonite are characteristic minerals in Yichang Gravel Layer while kyanite, garnet, rutile, monazite and magnetite are diagnostic minerals in the bedrocks. A-F): six typical sections of YGL, details in Fig. 4. G-H): Neogene bedrock (DDS) and Paleogene bedrock (PLK).

Figure 6. Left-hand panels: quartz ESR spectra of the Al and Ti centers of

present-day Yangtze River sediment from the Yichang area. Right-hand panels: magnified ESR spectra showing the quartz Ti–Li centers of present-day fluvial sediment from the Yangtze River in the Yichang area. The quartz Ti–Li centers are likely to have been bleached to zero prior to burial.

Figure 7. Additional dose response curves of quartz Ti–Li centers for samples collected from the Yichang Gravel, Jianghan Plain.

Figure 8. Map showing sampling sites for major rivers and bedrock in the Jianghan Basin. DDS-1: Duodaoshi Formation (bedrock); PLK-1: Pailoukou Formation (bedrock). Y-1~5: present-day Yangtze fluvial sediments in the Yichang area; H-1 and H-2: Hanjiang River; Q-1: Qing River; M-1: Manao River; J-1: Jushui River; Z-1: Zhanghe River (quoted from Kang et al., 2014).

Figure 9. Composition of the heavy mineral assemblage of the Yichang Gravel Layer (group of red triangles) and comparison of the assemblage with that of bedrocks (group of dark blue dots), present-day Yangtze fluvial sediments (group of light blue heart-shapes) and major rivers in the Jianghan Basin (group of yellow squares). All of the four ternary diagrams highlight that the heavy mineral assemblage of the YGL is similar to that of present-day Yangtze fluvial sediments, while is far distinct from that of bedrock and other rivers in Jianghan Plain. A): Ternary diagram based on the principle heavy minerals of zircon, apatite and leucoxene; B): Ternary diagram based on the principle heavy minerals of magnetite, ilmenite and tourmaline+kyanite; C):

Ternary diagram based on the principle heavy minerals. ATi: apatite%/(apatite%+tourmaline%); GZi: 100×garnet%/(garnet%+zircon%); ZTR: zircon%+tourmaline%+ rutile%; D): Ternary diagram based on the principle heavy minerals of epidote, hematite+limonite, and garnet+monazite (data of present-day Yangtze fluvial sediments and major rivers in the Jianghan Basin are quoted from Yang et al., 2009 and Kang et al., 2014).

Figure 10. Sketch map showing the valley and paleography evolution of the Three Gorges and Jianghan Basin in upper-middle Yangtze River Basin.

Figure 11. Lithology, paleomagnetic chronology, and provenance indicators variation of the Core Zhoulao (ZL) located in central Jianghan Basin. Magnetism characteristic, heavy mineral assemblage, pyroxenes content, and trace element characteristic revealed that the sediment from upper Yangtze River Basin had reached to Jinaghan Basin at about 1.1 Ma B.P. (Zhang et al., 2008; Kang et al., 2009; Yang et al., 2012; Yuan et al., 2012; Sun, 2018).

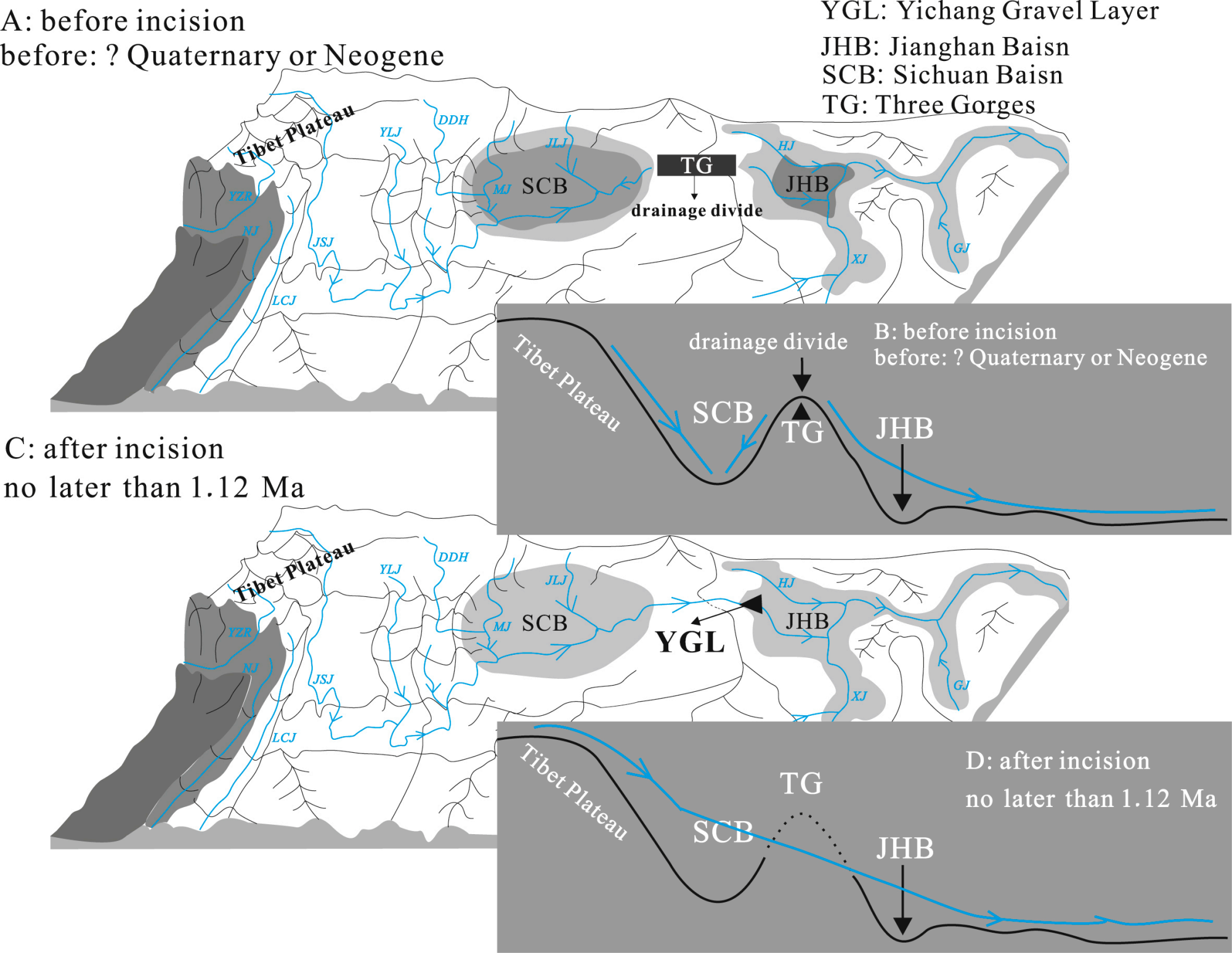
A: before incision
before: ? Quaternary or Neogene
YGL: Yichang Gravel Layer
JHB: Jianghan Baisn
SCB: Sichuan Baisn
TG: Three Gorges
Tibet Plateau
YLJ
DDH
JLJ
HJ
TG
drainage divide
MJ
SCB
JHB
YZR
NJ
JSJ
XJ
GJ
LCJ
B: before incision
before: ? Quaternary or Neogene
drainage divide
Tibet Plateau
SCB
TG
JHB
C: after incision
no later than 1.12 Ma
YGL
D: after incision
no later than 1.12 Ma